STABLE SOLUTION OF TIME DOMAIN INTEGRAL EQUATION METHODS USING QUADRATIC B-SPLINE TEMPORAL BASIS FUNCTIONS*

M. Y. Xia, G. H. Zhang and G. L. Dai

(*School of Electronics Engineering and Computer Science, Peking University, Beijing 100871, China
Email: myxia@pku.edu.cn, zgh@pku.edu.cn, daigaole_pku@126.com*)

C. H. Chan

(*Department of Electronic Engineering, City University of Hong Kong, Kowloon, Hong Kong, China
Email: eechic@cityu.edu.hk*)

Abstract

This paper is concerned with stable solutions of time domain integral equation (TDIE) methods for transient scattering problems with 3D conducting objects. We use the quadratic B-spline function as temporal basis functions, which permits both the induced currents and induced charges to be properly approximated in terms of completeness. Because the B-spline function has the least support width among all polynomial basis functions of the same order, the resulting system matrices seem to be the sparsest. The TDIE formulations using induced electric polarizations as unknown function are adopted and justified. Numerical results demonstrate that the proposed approach is accurate and efficient, and no late-time instability is observed.

Mathematics subject classification: 65N12, 65R20, 74S15.
Key words: TDIE methods, B-spline temporal basis functions, Transient scattering problems.

1. Introduction

Time domain integral equation (TDIE) methods have received much attention in several aspects in recent years, including stability, efficiency and application realms. Earlier studies of TDIE methods are concerned with the late-time instability [1-4] in transient scattering and radiation problems. The instability seriously impeded the popularity of the TDIE approaches. Fortunately, it has been found recently that this difficulty seems to be tractable by the proper choice of temporal basis functions [5-9]. The basis functions in [5-7] are compactly supported, while those in [8,9] are not which requires more memory and CPU time. In regarding to the efficiency of TDIE methods, the classical marching-on-in-time (MOT) scheme becomes more powerful by incorporating the fast Fourier transform (FFT) technique or plane wave time domain (PWTD) algorithm [10-13]. With the improvement of stability and efficiency, TDIE method is becoming a viable tool for simulation of complex microwave circuits containing nonlinear modules [12,13]. It is predicted that TDIE methods will have more applications for the wide-band analysis in many areas.

Though the TDIE method is likely to be the preferred solver for transient wave phenomenon, the stability problem is still a possible undermining factor, which is crucial for time domain simulation techniques. Although the use of the Lagrange interpolating temporal basis functions

---

[5,6] can produce stable solutions under the conventional MOT framework, the rationality of using these functions is still unjustified. In fact, the first-order derivatives of these basis functions are not continuous; consequently, the second-order derivatives do not exist. This question is raised because both the current and its derivatives are required to calculate the scattered fields. In contrast, there is a reasonable justification for employing the quadratic B-spline function as the temporal basis functions [7], which ensures that any unknown function and its derivatives up to the second order can be approximated by the basis functions and their derivatives, respectively. In addition, because the B-spline functions are most compactly supported among all the polynomial basis functions of the same order, the resulting system matrices seem to be the sparest. Unconditional stability of the TDIE methods with quadratic B-spline temporal basis functions for wire problems has been reported in [7], and the purpose of this work is to demonstrate its suitability to arbitrary 3D conducting objects.

In the following parts, various TDIE formulations are described in Section 2, and numerical demonstrations are provided in Section 3. Some concluding remarks are given in Section 4.

2. Formulation

Consider a transient wave which is incident upon a PEC (perfectly-electrical-conducting) object as shown in Fig. 2.1, which induces a distribution of electric polarization $\mathbf{P}_s$ on the surface S. The induced currents and charges on the surface are related to $\mathbf{P}_s(\mathbf{r}', t')$ through

$$\mathbf{J}_s(\mathbf{r}', t') = \partial \mathbf{P}_s(\mathbf{r}', t')/\partial t' \quad \text{and} \quad \sigma_s(\mathbf{r}', t') = -\nabla'_s \cdot \mathbf{P}_s(\mathbf{r}', t'),$$

so that the continuity equation is satisfied automatically, i.e.,

$$\nabla'_s \cdot \mathbf{J}_s(\mathbf{r}', t') + \partial \sigma_s(\mathbf{r}', t')/\partial t' = 0.$$

The vector potential and scalar potential generated by the induced sources are

$$\mathbf{A}(\mathbf{r}, t) = \frac{\mu_0}{4\pi} \int_S \frac{\mathbf{J}_s(\mathbf{r}', t - R/c)}{R} dS', \tag{2.1}$$

$$\phi(\mathbf{r}, t) = \frac{1}{4\pi\varepsilon_0} \int_S \frac{\sigma_s(\mathbf{r}', t - R/c)}{R} dS'. \tag{2.2}$$

The scattered fields can be expressed by the potentials as

$$\mathbf{E}^s = -\frac{\partial \mathbf{A}}{\partial t} - \nabla\phi = -\frac{1}{4\pi\varepsilon_0} \int_S \left[\frac{\partial^2 \mathbf{P}_s(\mathbf{r}', t - R/c)}{R\partial(ct)^2} - \nabla\frac{[\nabla'_s \cdot \mathbf{P}_s(\mathbf{r}', t')]_{t'=t-R/c}}{R} \right] dS', \tag{2.3}$$

$$\mathbf{H}^s = \frac{1}{\mu_0}\nabla \times \mathbf{A} = -\frac{1}{\eta_0}\frac{1}{4\pi\varepsilon_0} \int_S \frac{\hat{R}}{R} \times \left[\frac{\partial \mathbf{P}_s(\mathbf{r}', t - R/c)}{R\partial(ct)} + \frac{\partial^2 \mathbf{P}_s(\mathbf{r}', t - R/c)}{\partial(ct)^2} \right] dS', \tag{2.4}$$

where $c = 1/\sqrt{\varepsilon_0\mu_0}$ is the velocity of light in vacuum and $\eta_0 = \sqrt{\mu_0/\varepsilon_0}$ is the intrinsic impedance of the free space. The boundary conditions for a PEC surface are $\hat{n} \times (\mathbf{E}^i + \mathbf{E}^s) = \mathbf{0}$ and $\hat{n} \times (\mathbf{H}^i + \mathbf{H}^s) = \mathbf{J}_s = \partial \mathbf{P}_s/\partial t$, which by virtue of (2.3)-(2.4) become

$$\hat{n} \times \frac{1}{4\pi\varepsilon_0} \int_S \left[\frac{\partial^2 \mathbf{P}_s(\mathbf{r}', t - R/c)}{R\partial(ct)^2} - \nabla\frac{[\nabla'_s \cdot \mathbf{P}_s(\mathbf{r}', t')]_{t'=t-R/c}}{R} \right] dS' = n \times \mathbf{E}^i, \tag{2.5}$$

$$\frac{1}{2}\frac{\partial \mathbf{P}_s(\mathbf{r}, t)}{\partial t} + \hat{n} \times \frac{c}{4\pi}P.V.\int_S \frac{\hat{R}}{R} \times \left[\frac{\partial \mathbf{P}_s(\mathbf{r}', t - R/c)}{R\partial(ct)} \right.$$
$$\left. + \frac{\partial^2 \mathbf{P}_s(\mathbf{r}', t - R/c)}{\partial(ct)^2} \right] dS' = \hat{n} \times \mathbf{H}^i, \tag{2.6}$$
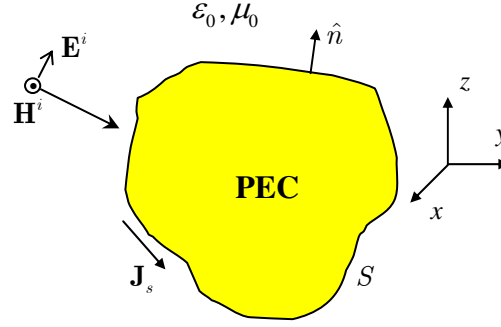
Fig. 2.1. Scattering by a 3D PEC object.

where $\mathbf{E}^i$ and $\mathbf{H}^i$ are the electric field and magnetic field of the incident wave. The P.V. in the second term of (2.6) means the Cauchy principal-value integral with the singularity at $R = 0$ removed and its contribution has been added to the first term.

Suppose that there is neither charge nor current distribution on the surface before the time instance $t' = 0$, which means that $\mathbf{P}_s(\mathbf{r}', t') = \partial \mathbf{P}_s(\mathbf{r}', t')/\partial t' = 0$ for $t' \leq 0$. Let $\mathbf{P}_s$ be expanded using the well-known RWG basis functions in the spatial domain and the quadratic B-spline functions in the time domain:

$$\mathbf{P}_s(\mathbf{r}', t') = (4\pi\varepsilon_0) \sum_{n=1}^{N} \sum_{j=0}^{\infty} P_n(j) S(\bar{t}' - j) \mathbf{f}_n(\mathbf{r}'), \tag{2.7}$$

where $\bar{t}' = t'/\Delta t$ and Δt is a prescribed resolution in the time axis, $\mathbf{f}_n(\mathbf{r}')$ for $n = 1, \cdots, N$ are the RWG basis functions [14] defined on the triangulated surface S. The current and charge distributions on the surface are

$$\mathbf{J}_s(\mathbf{r}', t') = \frac{4\pi\varepsilon_0}{\Delta t} \sum_{n=1}^{N} \sum_{j=0}^{\infty} P_n(j) S'(\bar{t}' - j) \mathbf{f}_n(\mathbf{r}'), \tag{2.8}$$

$$\sigma_s(\mathbf{r}', t') = (4\pi\varepsilon_0) \sum_{n=1}^{N} \sum_{j=0}^{\infty} P_n(j) S(\bar{t}' - j) g_n(\mathbf{r}'), \tag{2.9}$$

where $g_n(\mathbf{r}') = -\nabla' \cdot \mathbf{f}_n(\mathbf{r}')$. The quadratic B-spline function as plotted in Fig. 2.2 is expressed by

$$S(\bar{t}) = \begin{cases} \frac{1}{2}\bar{t}^2, 0 \leq \bar{t} < 1, \\ \frac{1}{2} + (\bar{t} - 1) - (\bar{t} - 1)^2, 0 \leq \bar{t} - 1 < 1, \\ \frac{1}{2} - (\bar{t} - 2) + \frac{1}{2}(\bar{t} - 2)^2, 0 \leq \bar{t} - 2 < 1. \end{cases} \tag{2.10}$$

Testing (2.5) with $\hat{n} \times \mathbf{f}_m(\mathbf{r})$ for $m = 1, \cdots, N$ and with (2.7) in place, we obtain

$$\sum_{j=0}^{\infty} \sum_{n=1}^{N} Z_{mn}^{\text{EFIE}}(\bar{t} - j) P_n(j) = E_m^i(\bar{t}), \tag{2.11}$$

with

$$Z_{mn}^{\text{EFIE}}(\bar{t}) = \int_{T_m} \int_{T_n} \frac{1}{R} \left[\frac{S(\bar{t} - \bar{R})}{(c\Delta t)^2} \mathbf{f}_m(\mathbf{r}) \cdot \mathbf{f}_n(\mathbf{r}') + S(\bar{t} - \bar{R}) g_m(\mathbf{r}) g_n(\mathbf{r}') \right] dS' dS, \tag{2.12}$$

$$E_m^i(\bar{t}) = \int_{T_m} \mathbf{f}_m(\mathbf{r}) \cdot \mathbf{E}^i(\mathbf{r}, \bar{t}\Delta t) dS, \tag{2.13}$$
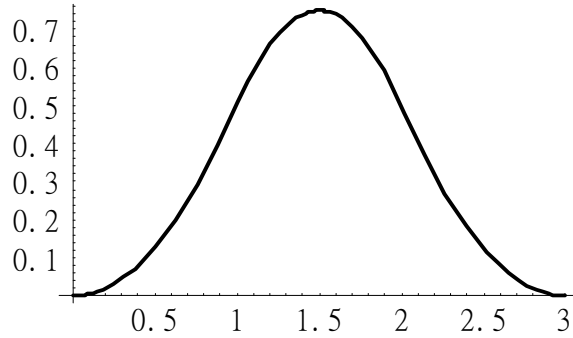
Fig. 2.2. The quadratic B-spline basis function.

where $\bar{t} = t/\Delta t$ and $\bar{R} = R/(c\Delta t)$. Testing (2.6) with $\eta_0 \mathbf{f}_m(\mathbf{r})$ for $m = 1, \cdots, N$, we have

$$\sum_{j=0}^{\infty} \sum_{n=1}^{N} Z_{mn}^{\mathrm{MFIE}}(\bar{t} - j) P_n(j) = \eta_0 H_m^i(\bar{t}), \tag{2.14}$$

with

$$Z_{mn}^{\mathrm{MFIE}}(\bar{t}) = \frac{2\pi}{c\Delta t} S'(\bar{t}) \int_{T_m} [\mathbf{f}_m(\mathbf{r}) \cdot \mathbf{f}_n(\mathbf{r})] dS$$

$$+ P.V. \int_{T_m} \int_{T_n} \frac{\mathbf{f}_m(\mathbf{r}) \cdot \hat{n} \times [\hat{R} \times \mathbf{f}_n(\mathbf{r}')]}{(c\Delta t)R} \left[\frac{S(\bar{t} - \bar{R})}{c\Delta t} + \frac{S'(\bar{t} - \bar{R})}{R} \right] dS' dS, \tag{2.15}$$

$$H_m^i(\bar{t}) = \int_{T_m} \mathbf{f}_m(\mathbf{r}) \cdot \hat{n} \times \mathbf{H}^i(\mathbf{r}, \bar{t}\Delta t) dS. \tag{2.16}$$

In this paper, we will use the electric polarization as unknown function, rather than using the induced current as unknown source. If the induced current is employed as unknown function, a temporal integral is required to find the induced charge and to evaluate the scalar potential [13,15]. To bypass this temporal integral, Eqs. (2.11) and (2.14) may be differentiated with respect to time [8,12]. This facilitates the solution for the unknown coefficients of the induced currents; however, the temporal integral is still unavoidable if the near-field computation is involved, such as in the analysis of electromagnetic compatibility or extraction of lumped parameters to construct equivalent circuit models. Another concern is whether the incident field or excitation source is indeed differentiable, say, in the case of a train of rectangular impulses denoting a digital signal. Instead, by using the electric polarization as unknown function, the charge and current are retrieved by derivatives which are normally evaluated easier than integrals, and the resulting system matrices are sparse as long as the expansion basis functions are compactly supported.

Applying the point matching method to (2.11) at $\bar{t} = i$ for $i = 1, 2, \cdots$, we arrive at

$$\sum_{j=j_{\min}}^{i-1} \sum_{n=1}^{N} Z_{mn}^{\mathrm{EFIE}}(i - j) P_n(j) = E_m^i(i), \quad i = 1, 2, \cdots, \tag{2.17}$$

where the upper limit is truncated at $j = i-1$ and the lower limit is from $j = j_{\min} = \max(0, i-L)$ due to the compactness of the temporal basis functions. Here $L = \mathrm{int}(R_{\max}/(c\Delta t) + 3)$ with $R_{\max}$ being the maximum linear dimension of the object, so that L is the number of time steps

within which a wave propagates a distance comparable to the dimension of the object. By changing the index $j \to i - j$, we obtain the MOT form based on the time domain electric field integral equation (TD-EFIE):

$$[Z^{\text{EFIE}}(1)]\{P(i-1)\} = \{E^i(i)\} - \sum_{j=2}^{\min(i,L)} [Z^{\text{EFIE}}(j)]\{P(i-j)\}, \tag{2.18}$$

where $[Z^{\text{EFIE}}(j)]$ for $j = 1, \cdots, L$ are matrices of size $N \times N$ with elements calculated by (2.12) at $\bar{t} = j$; $\{P(i-j)\}$ is a column vector of size $N \times 1$ associated with the $(i-j)$-th translated spline function; and $\{E^i(i)\}$ is a column vector of size $N \times 1$ with the elements given by (2.13).

Similarly, if matching (2.14) at $\bar{t} = i$ for $i = 1, 2, \cdots$, we obtain the MOT form based on the time domain magnetic field integral equation (TD-MFIE). The general MOT form based on the time domain combined field integral equation (TD-CFIE) is

$$[Z^{\text{CFIE}}(1)]\{P(i-1)\} = \{V^i(i)\} - \sum_{j=2}^{\min(i,L)} [Z^{\text{CFIE}}(j)]\{P(i-j)\} \tag{2.19}$$

with

$$[Z^{\text{CFIE}}(j)] = \alpha[Z^{\text{EFIE}}(j)] + (1 - \alpha)[Z^{\text{MFIE}}(j)], \tag{2.20}$$

$$\{V^i(i)\} = \alpha\{E^i(i)\} + (1 - \alpha)\{\eta_0 H^i(i)\}, \tag{2.21}$$

where $0 \leq \alpha \leq 1$ is a combination constant. If the object is open such as a conducting plate, $\alpha = 1$ must be used because the MFIE is not valid for open surfaces. For a closed object, an appropriate choice of α is necessary to suppress the resonant disturbance and increase the accuracy [16].

We emphasize that the integrals of (2.12) and (2.15) must be evaluated accurately, otherwise the MOT scheme may collapse due to error accumulation. The first integral of (2.15) can be evaluated analytically [15], while the second one is nonsingular and can be approximated accurately. As for the integral of (2.12), if $\bar{t} > 3$ it is nonsingular and can be evaluated numerically. For $\bar{t} \leq 3$, the singular integrals that we have to handle are of the form

$$\left\{ \begin{array}{c} I_1 \\ I_2 \end{array} \right\} = \int_{T_m} \int_{T_n} \left\{ \begin{array}{c} g_m(\mathbf{r})g_n(\mathbf{r}') \\ \mathbf{f}_m(\mathbf{r}) \cdot \mathbf{f}_n(\mathbf{r}') \end{array} \right\} \frac{dS'dS}{R}. \tag{2.22}$$

These two integrals, fortunately, have closed-form expressions if the double integrals are performed over the same triangle [17].

Finally, once the coefficients $\{P_n(j)\}_{j=0}^{N_t}$ are found, where N_t is the number of time sequence that has been resolved, the current may be retrieved by (2.8). The scattered far-field is the transverse components of the first term of (2.3), i.e.,

$$\mathbf{E}^s_{\text{far-zone}}(\mathbf{r}, t) = \hat{r} \times \hat{r} \times \frac{\partial \mathbf{A}}{\partial t}$$

$$\approx \frac{1}{r} \frac{1}{(c\Delta t)^2} \hat{r} \times \hat{r} \times \sum_{j=0}^{N_t} \sum_{n=1}^{N} P_n(j)\mathbf{F}_n(\bar{\tau} - j), \tag{2.23}$$

$$\mathbf{F}_n(\bar{\tau}) = \int_{T_n} S(\bar{\tau} + \hat{r} \cdot \mathbf{r}')\mathbf{f}_n(\mathbf{r}')dS', \tag{2.24}$$

where $\bar{\tau} = \bar{t} - \bar{r}$ is the retarded or far-field time-step with $\bar{r} = r/(c\Delta t)$ and $\bar{\mathbf{r}}' = \mathbf{r}'/(c\Delta t)$, and

$$\hat{r} = \hat{x}\sin\theta\cos\phi + \hat{y}\sin\theta\sin\phi + \hat{z}\cos\theta$$

with (θ, ϕ) indicating the scattering direction in a spherical coordinate system. Because $0 \leqslant \bar{\tau} - j + \hat{r}\cdot\bar{\mathbf{r}}' < 3$ due to the compactness of the temporal basis functions, we have

$$\bar{\tau} + (\hat{r}\cdot\bar{\mathbf{r}}')_{\min} - 3 < j \leqslant \bar{\tau} + (\hat{r}\cdot\bar{\mathbf{r}}')_{\max},$$

so that the terms of summation over the index j in (2.23) may be reduced greatly to speed up the computation of the scattered far-fields in a fixed direction at varying retarded instants. The radar cross-section (RCS) is usually defined in frequency domain. By converting the far-field data into frequency domain and normalized by the incident wave, we can obtain the wideband RCS for an object for one simulation run in the time domain.

3. Numerical Results

The incident wave used in this paper is the modulated Gaussian pulse [8]:

$$\mathbf{E}^i(\mathbf{r}, t) = \hat{u}\exp\left[-\left(\frac{\tau - t_0}{\sqrt{2}\sigma}\right)^2\right]\cos(2\pi f_0 \tau), \tag{3.1}$$

where f_0 is the centre carrier frequency and $\tau = t - \mathbf{r}\cdot\hat{k}/c$ with $\hat{u}$ and $\hat{k}$ indicating the polarization and incident directions; $t_0 = 8\sigma$ and $\sigma = 6/(2\pi f_{bw})$ with f_{bw} being the nominal bandwidth that the spectrum decays to about 1% at $f = f_0 \pm \frac{1}{2}f_{bw}$.

The first example is a square PEC plate with an edge size of $0.5m$ on the xy-plane and modeled with 1,407 unknowns using the RWG basis functions. Because this is an open-surface problem, the TD-EFIE must be adopted. For this example, $f_0 = 800$ MHz, $f_{bw} = 1600$ MHz and $\Delta t = 1/12$ ns have been used. Fig. 3.1(a) shows the evolution of induced current at the centre of the plate (LM=light meter: the time that light takes to travel $1m$). The late-time instability was not observed till the computation was terminated at 5,000 time-steps. The backscattered far-field computed by (2.23) is displayed in Fig. 3.1(b). Because the wideband RCS seems to be the most suitable quantity for validating the simulation data, the backscattering wideband RCS from zero frequency to 2.0GHz is plotted in Fig. 3.1(c). To check the accuracy, RCS data at a set of discrete frequency points are obtained using the MoM in the frequency domain, which coalesce with the TDIE results.

The second example is a PEC sphere of diameter $0.5m$, which is centered at the coordinate origin and modeled with 3,336 unknowns. For this closed body, because using either TD-EFIE or TD-MFIE alone may yield wrong wideband RCS at some frequencies due to interior resonant disturbance, the TD-CFIE has been employed. For this example, $f_0 = 700$ MHz, $f_{bw} = 1400$ MHz and $\Delta t = 1/12$ ns have been used. It is found that the MOT scheme is stable as show in Fig. 3.2(a). The backscattered far-field is presented in Fig. 3.2(b). The wideband RCS data are obtained from zero frequency to 1GHz, which are in good agreement with analytical MIE series solutions as shown in Fig. 3.2(c).

The last example is a metal cube of an edge size of $0.5m$, which is also centered at the coordinate origin and modeled with 2,592 unknowns. Also, the TD-CFIE has been adopted for this example to suppress the resonant disturbance. For this example, $f_0 = 650$ MHz, $f_{bw} = 1300$ MHz and $\Delta t = 1/12$ ns have been used. Again, no late-time instability has been observed as
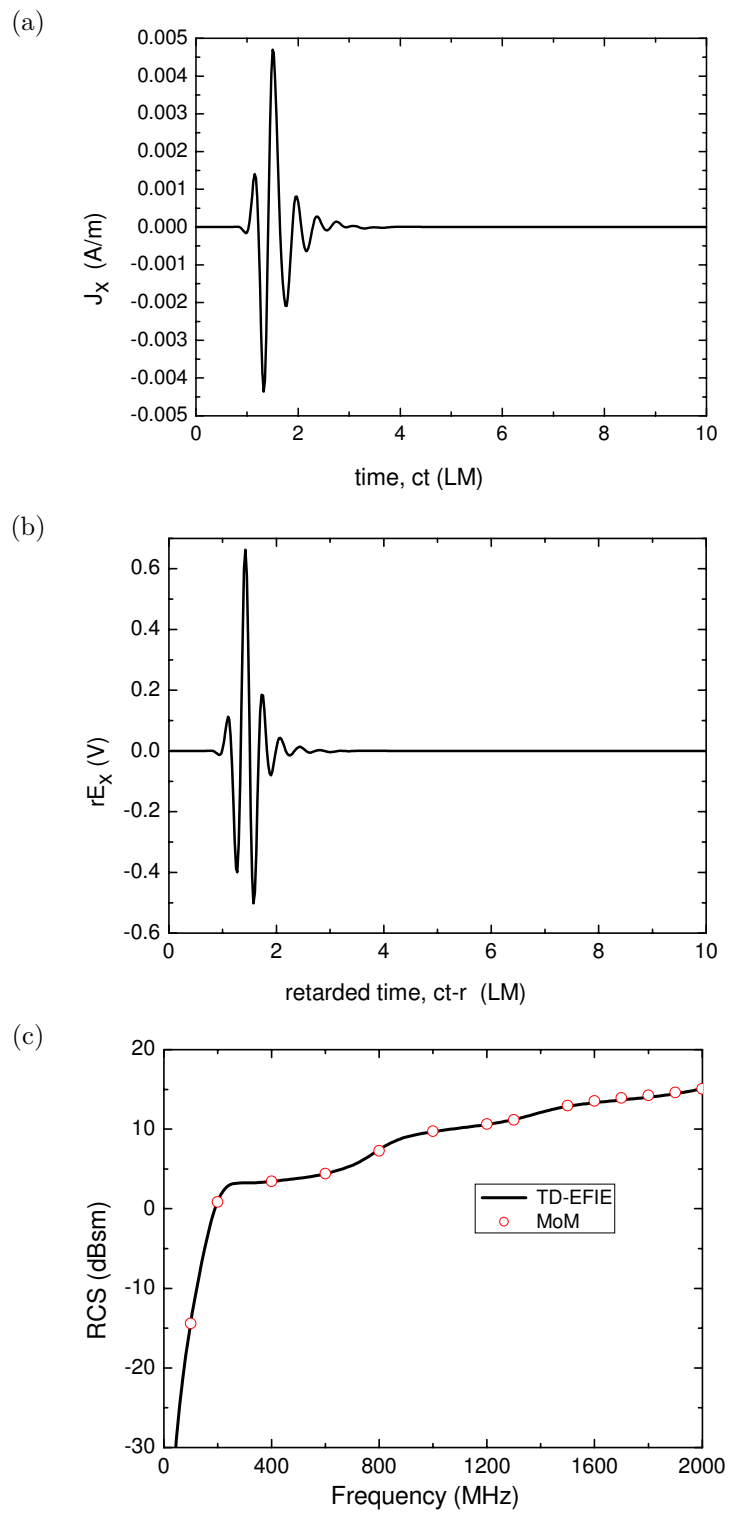
(a)

(b)

(c)

Fig. 3.1. Transient scattering of square PEC plate with an edge size of 0.5m: (a) induced currents at the centre, (b) backscattered far-fields, and (c) wideband backscattering RCS.
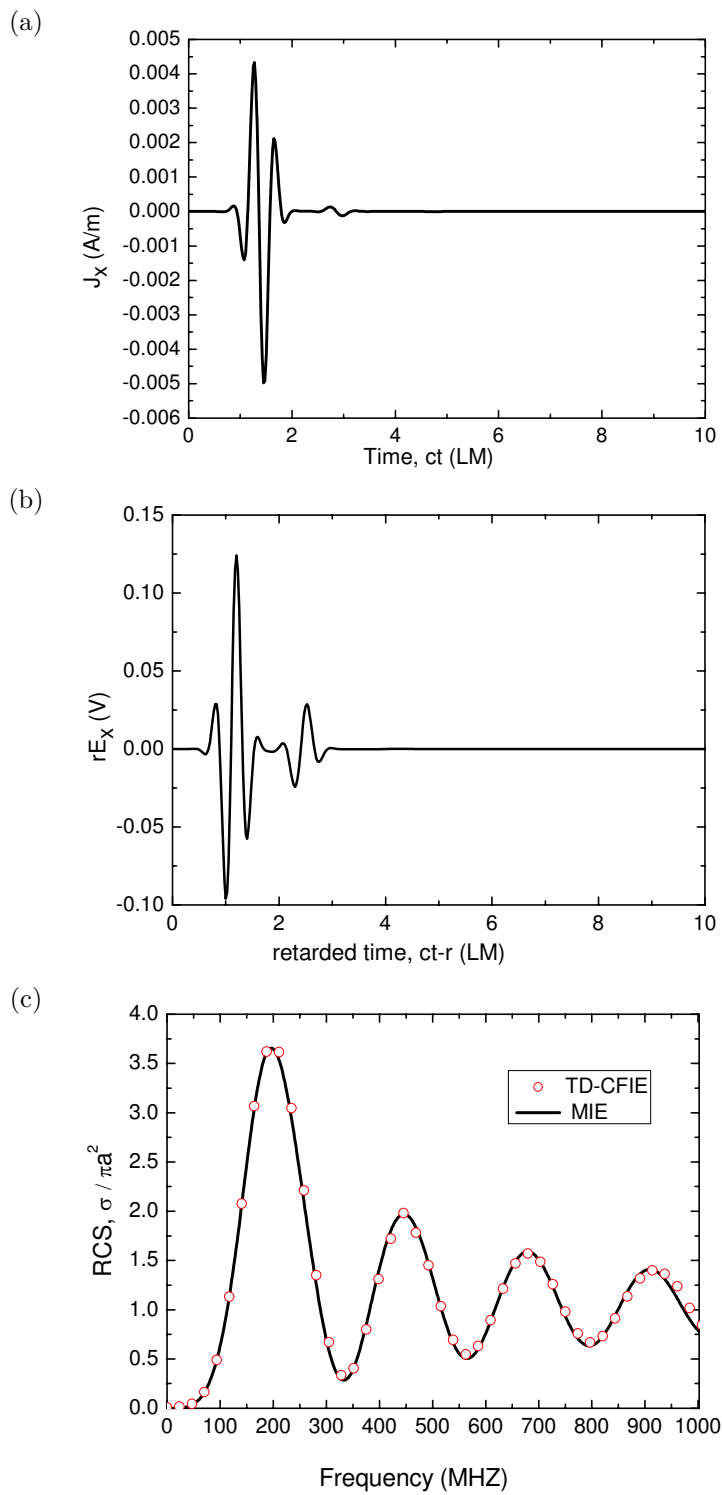
(a)

(b)

(c)

Fig. 3.2. Transient scattering of a PEC sphere with diameter of 0.5m: (a) induced currents at the pole pint, (b) backscattered far-field, and (c) wideband backscattering RCS.
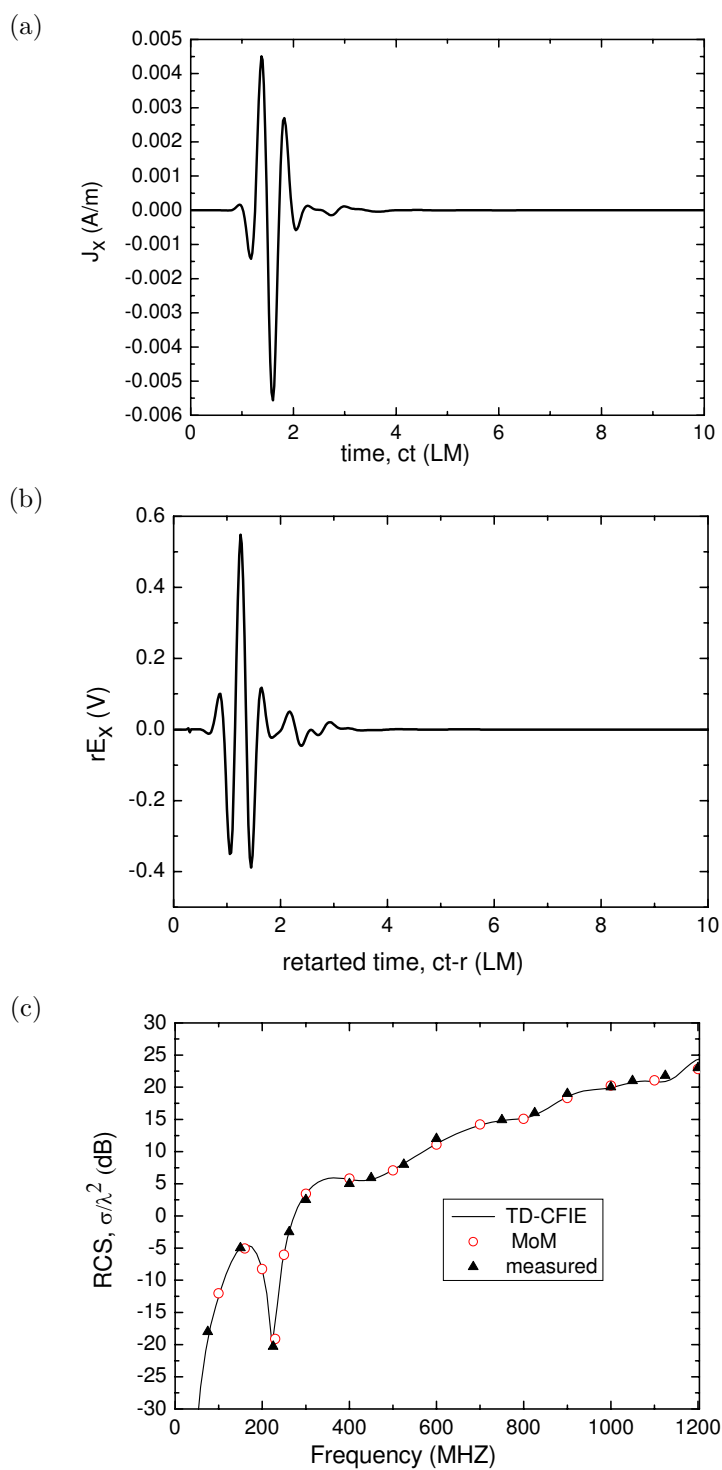
(a)

(b)

(c)

Fig. 3.3. Transient scattering of a PEC cube with edge size of 0.5m: (a) induced currents at the center of the top surface, (b) backscattered far-field, and (c) wideband backscattering RCS.

shown in Fig. 3.3(a). The backscattered far-field is provided in Fig. 3.3(b). The wideband backscattering RCS from 0 frequency to 1.2GHz are plotted in Fig. 3.3(c), which are found in good agreement with the MoM results and measured data [18].

4. Conclusions

A stable solution of the TDIE methods for transient scattering is investigated in this paper. The stability depends strongly on the choice of the temporal basis functions, in addition to the accurate evaluation of the matrix elements. The quadratic B-spline basis functions form a complete set up to the second order that permits both the induced current and induced charge to be properly represented. These basis functions are the most compact among all the polynomial basis functions of the same order. Consequently, the resulting system matrices seem to be the sparsest, which is important for storage of matrix elements and computation of matrix-vector multiplications in using MOT. Various TDIE formulations are derived by using the induced electric polarizations as updating quantities. Numerical results show that the proposed approach is accurate and efficient for wideband scattering problems with 3D conducting objects.

References

[1] D.A. Vechinski and S.M. Rao, A stable procedure to calculate the transient scattering by conducting surfaces of arbitrary shape, *IEEE T. Antenn. Propag.*, **40** (1992), 661-665.

[2] P.J. Davies and D.B. Duncan, Averaging techniques for time-marching schemes for retarded potential integral eequations, *Appl. Numer. Math.*, **23** (1997), 291-310.

[3] S. Dodson, S.P. Walker and M.J. Bluck, Implicitness and stability of time domain integral equation scattering analysis, *Appl. Comput. Electromagn. Soc. J.*, **13** (1998), 291-301.

[4] J.L. Hu, C.H. Chan and Y. Xu, A new temporal basis function for the time domain integral equation method, *IEEE Microw. Wirel. Compon. Lett.*, **11** (2001), 465-466.

[5] P.L. Jiang and E. Michielssen, Temporal acceleration of time-domain integral equation solvers for electromagnetic scattering from objects residing in lossy media, *Microw. Opt. Techn. Lett.*, **44** (2005), 223-230.

[6] H. Bagci, A.E. Yilmaz, V. Lomakin and E. Michielssen, Fast solution of mixed-potential time-domain integral equations for half-space environments, *IEEE T. Geosci. Remote Sensing*, **43** (2005), 269-279.

[7] M.Y. Xia, G.H. Zhang, P. Wang and C.H. Chan, Time domain integral equation method for transient analysis of wires using quadratic B-spline as temporal basis functions, *IEEE T. Antenn. Propag.*, under review.

[8] D.S. Weile, G. Pisharody, N.-W. Chen, B. Shanker and E. Michielssen, A novel scheme for the solution of the time-domain integral equations of electromagnetics, *IEEE T. Antenn. Propag.*, **52** (2004), 283-295.

[9] Y.S. Chung, T.K. Sarka, B.H. Jung, M.S. Palma, Z. Ji, S. Jang and K. Kim, Solution of time domain electric field integral equation using the Laguerre polynomials, *IEEE T. Antenn. Propag.*, **52** (2004), 2319-2328.

[10] J.L. Hu, C.H. Chan and Y. Xu, A fast solution of time domain integral equation using fast Fourier transformation, *Microw. Opt. Techn. Lett.*, **25(3)** (2000), 172-175.

[11] B. Shanker, A.A. Ergin, M. Lu and E. Michielssen, Fast analysis of transient electromagnetic scattering phenomena using the multilevel plane wave time domain algorithm, *IEEE T. Antenn. Propag.*, **51** (2003), 628-641.

[12] K. Aygun, B.C. Fischer, J. Meng, B. Shanker and E. Michielssen, A fast hybrid field-circuit simulator for transient analysis of microwave circuits, *IEEE T. Microw. Theory Tech.*, **52** (2004), 573-583.

[13] A.E. Yilmaz, J.M. Jin and E. Michielssen, A parallel FFT accelerated transient filed-circuit simulator, *IEEE T. Microw. Theory Tech.*, **53** (2005), 2851-2864.

[14] S.M. Rao, D.R. Wilton and A.W. Glisson, Electromagnetic scattering by surfaces of arbitrary shape, *IEEE T. Antenn. Propag.*, **30** (1982), 409-418.

[15] S.M. Rao and T.K. Sarker, Numerical solution of time domain integral equation for arbitrarily shaped conductor/dielectric composite bodies, *IEEE T. Antenn. Propag.*, **50** (2002), 1831-1837.

[16] B. Shanker, A.A. Ergin, K. Aygun and E. Michielssen, Analysis of transient electromagnetic scattering from closed surfaces using a combined field integral equation, *IEEE T. Antenn. Propag.*, **48** (2000), 1064-1074.

[17] P. Arcioni, M. Bressan and L. Perregrini, On the evaluation of the double surface integrals arising in the application of the boundary integral method to 3-D problems, *IEEE T. Microw. Theory Tech.*, **45** (1997), 436-438.

[18] M.G. Cote, M.B. Woodworth and A.D. Yaghjian, Scattering from the perfectly conducting cube, *IEEE T. Antenn. Propag.*, **36** (1988), 1321-1329.